Mon. Not. R. Astron. Soc. **000**, 1–15 (2010) Printed 14 July 2010 (MN LATEX style file v2.2)

Early-type galaxies in different environments: an H I view

Tom Oosterloo[1,2⋆], Raffaella Morganti[1,2], Alison Crocker[3,4]†, Eva Jütte[1,5], Michele Cappellari[3], Tim de Zeeuw[6,7], Davor Krajnović[3,6], Richard McDermid[8], Harald Kuntschner[9], Marc Sarzi[10], Anne-Marie Weijmans[7,11]

[1] *ASTRON - Netherlands Institute for Radio Astronomy, Postbus 2, 7990 AA Dwingeloo, The Netherlands*
[2] *Kapteyn Astronomical Institute, University of Groningen Postbus 800, 9700 AV Groningen, The Netherlands*
[3] *Sub-department of Astrophysics, University of Oxford, Denys Wilkinson Building, Keble Road, Oxford OX1 3RH*
[4] *Department of Astronomy, University of Massachusetts, 710 North Pleasant Street Amherst, MA 01003-9305 USA*
[5] *Astronomisches Institut, Ruhr-Universität Bochum, Universitätsstrasse 150, D-44801 Bochum, Germany*
[6] *European Southern Observatory, Karl-Schwarzschild Strasse 2, 85748 Garching bei München, Germany*
[7] *Sterrewacht Leiden, Universiteit Leiden, Niels Bohrweg 2, 2333 CA Leiden, The Netherlands*
[8] *Gemini Observatory, 670 N. A'ohoku Place, Hilo, Hawaii 96720 USA*
[9] *Space Telescope European Coordinating Facility, Karl-Schwarzschild-Str. 2, D-85748 Garching bei München, Germany*
[10] *Centre for Astrophysics Research, Science & Technology Research Institute, University of Hertfordshire, Hatfield, United Kingdom*
[11] *Dunlap Institute for Astronomy & Astrophysics, University of Toronto, 50 St. George Street, Toronto, ON M5S 3H4, Canada*

Accepted 2010 July 12. Received 2010 July 7 ; in original form 2010 March 5

ABSTRACT

We present an analysis of deep Westerbork Synthesis Radio Telescope observations of the neutral hydrogen in 33 nearby early-type galaxies selected from a representative sample studied earlier at optical wavelengths with the *SAURON* integral-field spectrograph. This is the deepest homogeneous set of H I imaging data available for this class of objects. The sample covers both field environments and the Virgo cluster. Our analysis shows that gas accretion plays a role in the evolution of field early-type galaxies, but less so for those in clusters.

The H I properties of *SAURON* early-type galaxies strongly depend on environment. For detection limits of a few times 10^6 $M_\odot$, H I is detected in about 2/3 of the field galaxies, while <10% of the Virgo objects are detected. In about half of the detections, the H I forms a regularly rotating disc or ring. In many galaxies unsettled tails and clouds are seen. All H I discs have counterparts of ionised gas and inner H I discs are also detected in molecular gas. The cold ISM in the central regions is dominated by molecular gas ($M_{\rm H_2}/M_{\rm HI} \simeq 10$). Assuming our sample is representative, we conclude that accretion of H I is very common for field early-type galaxies, but the amount of material involved is usually small and the effects on the host galaxy are, at most, subtle. Cluster galaxies appear not to accrete H I, or the accreted material gets removed quickly by environmental effects. The relation between H I and stellar population is complex. The few galaxies with a significant young sub-population all have inner gas discs, but for the remaining galaxies there is no trend between stellar population and H I properties. A number of early-type galaxies are very gas rich, but only have an old population. The stellar populations of field galaxies are typically younger than those in Virgo. This is likely related to differences in accretion history. There is no obvious overall relation between gas H I content and global dynamical characteristics except that the fastest rotators all have an H I disk. This confirms that if fast and slow rotators are the result of different evolution paths, this is not strongly reflected in the *current* H I content. In about 50% of the galaxies we detect a central radio continuum source. In many objects this emission is from a low-luminosity AGN, in some it is consistent with the observed star formation. Galaxies with H I in the central regions are more likely detected in continuum. This is due to a higher probability for star formation to occur in such galaxies and not to H I-related AGN fuelling.

Key words: galaxies: elliptical and lenticular, cD — galaxies: evolution

⋆ E-mail:oosterloo@astron.nl † ASTRON/JIVE Summer Student 2007

1 INTRODUCTION

One of the central topics in current extra-galactic astronomy is how early-type galaxies form and how their properties change through cosmic times. This is a particularly difficult task as this class of objects shows a diversity in its properties that goes beyond present-day simulations. The generally accepted framework is that early-type galaxies form in a hierarchical way through the accretion and merging of smaller systems. Although hierarchical growth in itself is a relatively simple premise, the details of early-type galaxy formation and evolution are very complex and depends on a large number of parameters which is likely the reason for the observed variety of the final galaxies.

One of the main issues is how much gas is involved in the accretion/merging process and to what extent it involves approximately equal-mass systems or the accretion of small companions. Theoretical work has shown that the amount of gas involved in the growth of early-type galaxies can be a major factor, in particular in determining the morphological and dynamical structure of early-type galaxies. For example, more anisotropic and slowly rotating galaxies would result from predominantly collisionless major mergers, while faster rotating galaxies are produced by more gas-rich mergers and accretions. The inner structure (i.e. cores vs cusps) is also likely related to the type of merger/accretion (e.g. Bender, Burstein, & Faber 1992; Jesseit, Naab, & Burkert 2005; Naab, Jesseit, & Burkert 2006; Hopkins et al. 2009; Jesseit et al. 2009).

Some arguments suggest that the evolution of early-type galaxies is 'dry', i.e. gas does not play an important role. The basic argument is that the amount of stars in red galaxies has at least doubled since $z = 1$, while the red colours of early-type galaxies indicate that they are dominated by old stars. This indicates that the growth since $z = 1$ is dry, i.e. it is not accompanied with much star formation (e.g. Bell et al. 2004; van Dokkum 2005; Tal et al. 2009).

While this may suggest that globally the amount of gas involved since $z = 1$ is at most modest, several observational studies, touching on several topics, show that gas does play at least some role. For example, stellar-population studies show that many systems do contain a (often small) sub-population of relatively young stars that may have formed from accreted gas (e.g. Trager et al. 2000; Tadhunter et al. 2005; Yi et al. 2005; Serra et al. 2006; Serra et al. 2008; Kaviraj et al. 2010). Similarly, early work by, e.g., Malin & Carter (1983) and Schweizer & Seitzer (1992), has shown that direct morphological signs of accretion are observed in a large fraction of early-type galaxies and that such signs correlate with the presence of a young stellar sub-population, indicating the presence of gas in these accretions. More recent work has shown that this is also the case for samples of early-type galaxies that originally seemed to support the dry-merging hypothesis (Donovan, Hibbard, & van Gorkom 2007; Sánchez-Blázquez et al. 2009; Serra & Oosterloo 2010). Dynamically distinct stellar and gaseous subcomponents are often found in early-type galaxies. In many cases, such sub-components are both chemically and kinematically distinct (McDermid et al. 2006), strongly suggesting that external gas has entered the system. The orbital structure of fast-rotating early-type galaxies also seems to indicate that gas was involved in their evolution (Emsellem et al. 2007; Cappellari et al. 2007). Finally, the tight scaling relations found for early-type galaxies place a rather conservative upper limit on the fraction of stellar mass assembled via dissipationless merging (e.g. Nipoti, Londrillo, & Ciotti 2003; Nipoti, Treu, & Bolton 2009).

Recently, also *direct evidence* for the importance of gas has been found. Early-type galaxies in the nearby Universe used to be generally perceived to be gas poor. Although indeed they typically have less cold gas than spiral galaxies, it is now becoming clear that cold gas is present perhaps most of them, in particular those in the field. For example, for a detection limit of a few $\times 10^7\ M_\odot$, molecular gas is detected in at least a quarter of early-type galaxies (Welch & Sage 2003; Sage, Welch, & Young 2007; Combes et al. 2007; Young et al. 2010). Recent work on the neutral hydrogen in early-type galaxies suggests that, in terms of detection limits of a few times $10^6\ M_\odot$, about half the field early-type galaxies are detected (Morganti et al. 2006; Grossi et al. 2009; Serra et al. 2009). The H I datacubes obtained by Morganti et al. (2006) also show, in terms of the characteristics of the neutral hydrogen detected, the class of field early-type galaxies appears to be rich and varied, much more so than spirals.

An interesting aspect is that early-type galaxies in clusters appear to have different gas properties from those in the field (di Serego Alighieri et al. 2007; Serra et al. 2009). Therefore, if gas plays a role in the evolution of early-type galaxies, this should become visible by comparing properties of cluster early-type galaxies with those of objects in the field.

In this paper we expand on the results obtained in Morganti et al. (2006) with particular focus on the effect of environment. We present deep H I imaging observations for 22 galaxies selected from the *SAURON* sample (de Zeeuw et al. 2002) where we have, in contrast to Morganti et al. (2006), also selected galaxies from the Virgo cluster. Combining these new data with those of Morganti et al. (2006) resulted in deep H I data for 33 *SAURON* galaxies north of declination $+10^\circ$. This is the largest and deepest collection of H I imaging data available for early-type galaxies. The *SAURON* sample is well suited for a detailed comparison between field and cluster galaxies: for all *SAURON* galaxies a wealth of information is available, including 3-D spectroscopy of the stars and of the ionised gas as well as data obtained in many other wavebands. A potential concern is that in principle the H I properties were part of the selection of the *SAURON* sample. However, in practise this affected the selection of only a few objects of the *SAURON* sample of 48 early-type galaxies. Importantly, the selection was done independent of environment. Therefore, results based on a comparison of the H I properties of *SAURON* galaxies in different environments should be robust.

The paper is organised in the following way. We describe the sample selection and the observations in Section 2. In Section 3 we present the results for the new H I detected galaxies. In Section 4 we discuss the observed H I properties of early-type galaxies in the context of their evolution.

2 SAMPLE SELECTION AND H I OBSERVATIONS

We observed 22 galaxies from the *SAURON* sample (de Zeeuw et al. 2002) with the Westerbork Synthesis Radio Telescope (WSRT). For one of these galaxies (NGC 4486/M87), the very strong radio continuum emission prevented us to obtain a data cube of good enough quality. This object is, therefore, excluded from the analysis. As mentioned above, the newly observed galaxies expand the sample presented in Morganti et al. (2006) with objects down to the declination limit of $+10^\circ$ and including galaxies that are member of the Virgo cluster. Lowering the declination limit is a compromise between increasing the sample size while maintaining good image quality. For galaxies close to the declination limit, due to the east-west layout of the WSRT, the beam elongation be-

NGC	$V_{\rm centr}$ km s^{-1}	D Mpc	pc/″	Date	Int.Time h	Beam ″ × ″ (°)	Noise H I mJy beam^{-1}	Noise Cont. mJy beam^{-1}	H I contours 10^{19} cm^{-2}
(1)	(2)	(3)	(4)	(5)	(6)	(7)	(8)	(9)	(10)
524	2379	23.3	113		3×12	85×23	0.28	0.062	1,2
821	1742	23.4	113		4×12	72×13	0.20	0.050	–
3032	1561	21.4	104		4×12	43×25	0.19	0.048	2, 5, 10, 20, 50
3377	698	10.9	53		12	73×24	0.37	0.053	–
3379	877	10.3	50		12	73×24		0.052	–
3384	729	11.3	55		12	73×24		0.052	1, 2, 5
3489	688	11.7	57		4×12	76×25	0.20	0.047	0.5, 1, 2, 5, 10
3608	1201	22.3	108		4×12	62×22	0.22	0.043	2, 5
4262	1361	15.4	75		12	68×24	0.42	0.069	10, 20, 50
4374	1016	18.5	90		12	59×26	0.72		–
4382	745	17.9	87		12	59×26	0.39	0.062	–
4387	550	17.9	87		12	67×24	0.45	0.490	–
4458	676	16.4	79		12	71×25	0.41	0.128	–
4459	1182	16.1	78		12	69×25	0.40	0.065	–
4473	2210	15.3	s 74		12	71×25	0.42	0.151	–
4477	1327	16.5	80		12	71×25	0.38	0.124	–
4486	1272	17.2	83		12	–	–	–	–
4550	407	15.5	75		12	74×25	0.39	0.121	–
4552	288	15.8	77		12	78×24	0.60	0.098	–
4564	1116	15.8	77		12	76×25	0.68	0.144	–
4621	431	14.9	72		12	76×25	0.39	0.073	–
4660	1082	15.0	73		12	77×25	0.39	0.059	–

Table 1. Summary of the observations of the galaxies in the sample. (1) Galaxy identifier. (2) Systemic velocity at which we centred the H I observation band. (3) Galaxy distance (Tonry et al. 2001, corrected by subtracting 0.06 mag, see Mei et al. (2005)), Tully (1988) or from the LEDA database assuming a Hubble flow with $H_\circ = 75$ km s^{-1} Mpc^{-1}. (4) Linear scale. (5) Date of observation. (6) Integration time in hours. (7) Beam size. (8) Noise level in the H I cube (natural). (9) Noise level of the continuum image. (10) Contour levels of the total intensity images shown in Fig. 1.

comes significant, and spatially resolved information becomes limited. However, given that most of the H I structures detected so far are very extended and of low surface brightness, the large WSRT beam is not a major disadvantage. For the observations, a single observing band of 20 MHz (corresponding to ~ 4000 kms^{-1}), centred on the systemic velocity of the target, and 1024 channels for both polarisations was used. All observations were done with the maxi-short antenna configuration. In most cases, we observed the targets for 12 h. For five objects that turned out to have interesting but faint H I detections, or for which the single 12-h observation gave a tentative detection, follow up observations (3×12h) were obtained. The details of the observations are given in Table 1.

The calibration and analysis were done using the *MIRIAD* package (Sault, Teuben, & Wright 1995). The data cubes were constructed with a robust weighting equal to 0 (Briggs 1995). In the cases where faint, extended structures were detected (e.g. NGC 3489), additional cubes were constructed using natural weighting. The cubes were made by averaging channels in groups of two, followed by Hanning smoothing, resulting in a velocity resolution of 16 km s^{-1}. This was done to match the spectral resolution to the expected line widths. The r.m.s. noise and restoring beam sizes of each cube are given in Table 1. For reference: a beam size of 1 arcminute corresponds to about 5 kpc for a galaxy at a distance of 15 Mpc.

The line-free channels were used to obtain an image of the radio continuum of each galaxy. The continuum images were made with uniform weighting. The r.m.s. noise and beam of these images are also given in Table 1. Radio continuum emission was not detected in 14 of the objects. All detected continuum sources are unresolved.

3 RESULTS

Neutral hydrogen is detected in our new observations in, or near, six galaxies. Some details about the individual detections are given at the end of this section. Five of the detections are of H I in field early-type galaxies (out of 8 field galaxies observed), one is in a galaxy that is a member of the Virgo cluster (out of 13 Virgo galaxies observed). Figure 1 shows the H I total intensity images of the detections. In the strongest detections - NGC 3032, NGC 3489, NGC 4262 - the H I is located in a regular disc/ring-like structure, which in the case of NGC 3489 connects to a long low-surface brightness tail of H I.

In NGC 3608, the H I is detected about $\sim$ 12 arcmin (corresponding to $\sim$ 70 kpc) from the galaxy, at a velocity close to the systemic velocity of NGC 3608 and without any obvious optical counterpart. A few other (also early-type) galaxies are nearby so it is difficult to assign the H I to NGC 3608 unambiguously. A fifth H I detection is NGC 3384. Together with NGC 3377 and NGC 3389, this galaxy is surrounded by the well-known Leo Ring (Schneider et al. 1983; Schneider 1989) of which we conclude that at least one H I cloud is likely associated with NGC 3384. Finally, in NGC 524 we detect a small H I cloud near the edge of the optical body. The results for the field galaxies, with regard to both morphology and detection rate, are in line with those we obtained in our previous study of *SAURON* galaxies (Morganti et al. 2006).

A clear result is that Virgo early-type galaxies clearly have different H I properties than field galaxies. This is discussed in more detail in Secs 4.1 and 4.6. For galaxies where no H I was detected, the upper limits on the H I mass were calculated as three times the statistical error of a signal with a width of 200 km s^{-1} over one synthesised beam. The upper limits of the H I mass range from a few times 10^6 $M_\odot$ to 3×10^7 $M_\odot$. The quantitative results

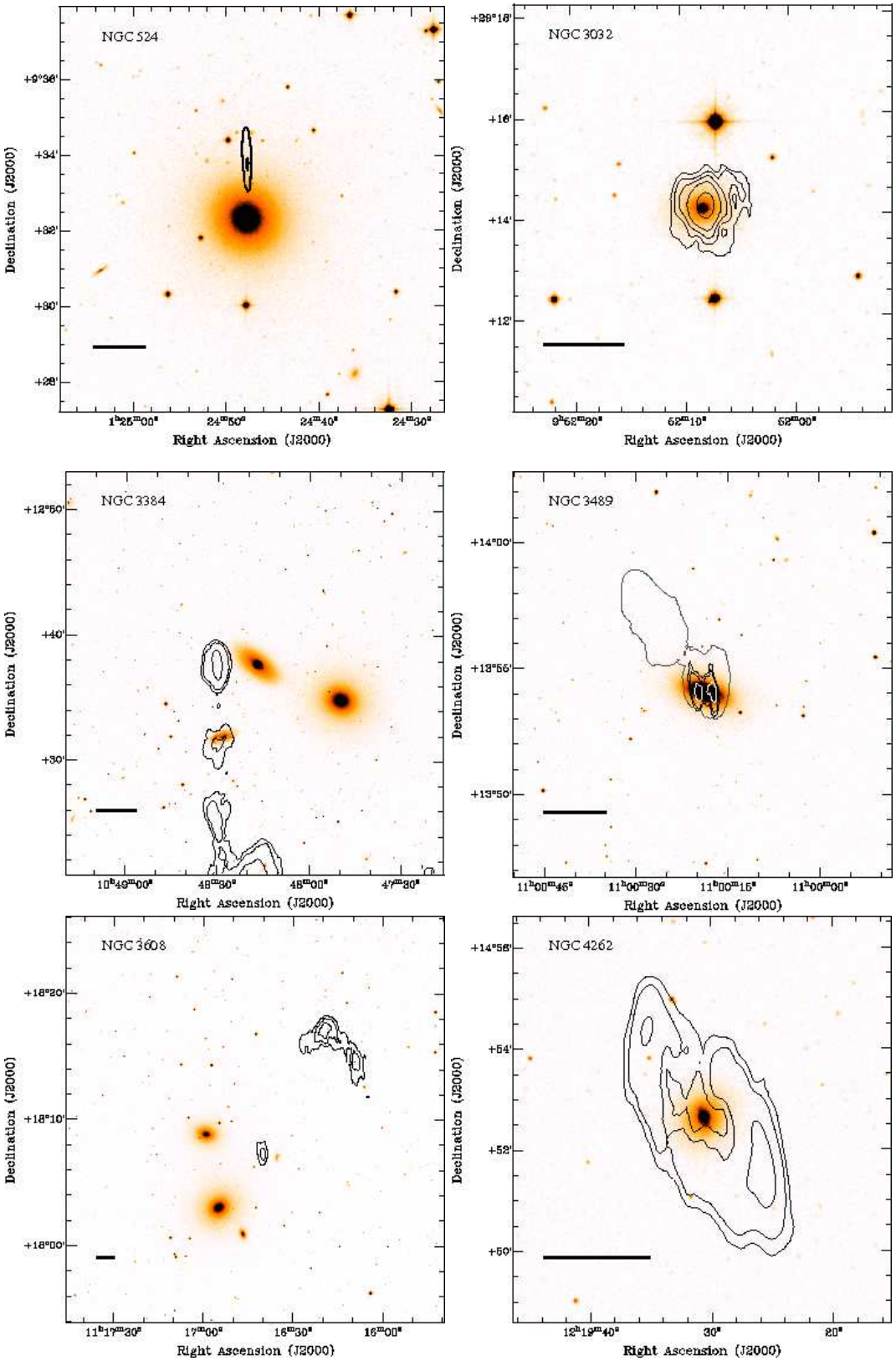

Figure 1. Total H I intensity images (contours) superimposed onto Digital Sky Survey optical images of the newly detected objects - NGC 524, NGC 3032, NGC 3384 (part of the Leo Ring), NGC 3489, NGC 3608 and NGC 4262. The contour levels are given in Table 1. The horizontal bar in each panel indicates 10 kpc. Total H I intensity image for NGC 3384 has been made excluding the high-velocity system belonging to ¡NGC 3389 (see text)

NGC	Type	$M_{\rm HI}$ $M_\odot$	$M_{\rm HI}/L_B$	H I morph	Env	$S_{1.4\rm GHz}$ mJy	$\log P_{1.4\rm GHz}$ W/Hz
(1)	(2)	(3)	(4)	(5)	(6)	(7)	(8)
524	S0	2.6×10^6	0.000045	C	F	2.19	20.13
821	E	$<4.4 \times 10^6$	<0.00018	N	F	<0.15	<18.97
3032	S0	9.6×10^7	0.019	D	F	5.66	20.47
3377	E	$<1.8 \times 10^6$	<0.00023	N	F	<0.16	<18.33
3379	E	$<1.8 \times 10^6$	<0.0001	N	F	0.87	19.02
3384	S0	1.2×10^7	0.00116	C	F	<0.16	<18.35
3489	S0	5.8×10^6	0.00007	D	F	1.22	19.28
3608	E	2.5×10^6	0.00024	C	F	0.5	19.45
4262	S0	6.4×10^8	0.115	D	C	0.71	19.28
4374	E	$<9.3 \times 10^6$	<0.00019	N	C	1500	22.8
4382	S0	$<5.0 \times 10^6$	<0.0001	N	C	<0.19	<18.83
4387	E	$<1.2 \times 10^7$	<0.0037	N	C	<1.47	<19.73
4458	E	$<4.6 \times 10^6$	<0.00126	N	C	<0.38	<19.07
4459	S0	$<3.9 \times 10^6$	<0.00025	N	C	1.52	19.65
4473	E	$<3.9 \times 10^6$	<0.0002	N	C	<0.45	<19.08
4477	S0	$<4.1 \times 10^6$	<0.00027	N	C	1.16	19.55
4550	S0	$<3.7 \times 10^6$	<0.0007	N	C	<0.36	<18.85
4552	E	$<5.3 \times 10^6$	<0.00020	N	C	84.1	21.38
4564	E	$<5.8 \times 10^6$	<0.00065	N	C	<0.43	<19.09
4621	E	$<4.9 \times 10^6$	<0.00018	N	C	<0.22	<18.74
4660	E	$<2.4 \times 10^6$	<0.00031	N	C	<0.18	<18.65
1023	S0	2.1×10^9	0.046	A	F	0.4	18.7
2549	S0	$<2.0 \times 10^6$	<0.00043	N	F	<0.1	<18.3
2685	S0	1.8×10^9	0.27	D	F	2	19.8
2768	E	1.7×10^8	0.0038	A	F	10.9	20.8
3414	S0	1.6×10^8	0.0096	D	F	5.0	20.6
4150	S0	2.5×10^6	0.00078	D	F	0.8	19.2
4278	E	6.9×10^8	0.039	D	F	336.5	22.0
5198	E	6.8×10^8	0.030	A	F	2.4	20.6
5308	S0	$<1.5 \times 10^7$	<00064	N	F	<0.24	<19.5
5982	E	3.4×10^7	0.00060	C	F	0.5	20.1
7332	S0	6.0×10^6	0.00038	C	F	<0.13	<18.9
7457	S0	$<2.0 \times 10^6$	<0.00032	N	F	<0.11	<18.5

Table 2. Measurements based on our radio observations. The top part of this table is based on the observations presented here. For completeness, we include the parameters from Morganti et al. (2006). (1) Galaxy identifier. (2) Hubble type (NED). (3) Total H I mass. (4) Ratio of total H I mass and the absolute B-band luminosity L_B. (5) Code describing H I morphology: N: not detected, C: isolated cloud, A: accretion, D: disc (6) Environment code: F: field, C: Virgo cluster (7) Continuum flux (or 3σ upper limits) at 1.4 GHz. (8) Total radio power at 1.4 GHz.

are given in Table 2. Since we will discuss the H I results for all *SAURON* galaxies observed, we also include the parameters of the galaxies observed by Morganti et al. (2006).

The H I masses of the newly detected objects range between 10^7 $M_\odot$ to a few times 10^8 $M_\odot$. The relative gas content ($M_{\rm HI}/L_{\rm B}$) ranges from $<$ 0.0001 $M_\odot/L_\odot$ to 0.115 $M_\odot/L_\odot$. Typical values for $M_{\rm HI}/L_{\rm B}$ for spiral galaxies, depending on type and luminosity, range from 0.1 $M_\odot/L_\odot$ to above 1.0 $M_\odot/L_\odot$ (Roberts & Haynes 1994). These values underline the well-known fact that early-type galaxies are H I poor relative to spiral galaxies. The sizes of the H I structures observed in this sample vary between a few kpc up to ∼40 kpc. Figure 1 shows that the peak column density istypically at most a few times 10^{20} cm^{-2}. As already found in many earlier studies (e.g. van Driel & van Woerden 1991; Morganti et al. 1997, 2006; Serra et al. 2006; Oosterloo et al. 2007), these column densities are lower than the critical surface density for star formation (Kennicutt 1989; Schaye 2004; Bigiel et al. 2008). Although this result implies the absence of widespread star formation activity, given the relatively low spatial resolution of our data, the column density will be above the star formation threshold in local, small regions and some star formation can be expected.

Before we further discuss the possible implications of our H I observations, we summarise the H I characteristics for the individual objects detected.

NGC 524 - We detect a small H I cloud in the outer regions of this galaxy. Possibly this corresponds to a small gas-rich companion, although no direct optical counterpart is visible on fairly deep optical images (Jeong et al. 2009). A small galaxy, of which the redshift is not known, is seen about 1 arcmin from the H I cloud. Possibly a small companion is stripped from its H I by NGC 524, in a similar way as is occurring in, e.g., NGC 4472 (McNamara et al. 1994). NGC 524 has a weak disc of ionised gas which rotates with the same sense as the stars (Sarzi et al. 2006). This disc is also detected in CO with an implied molecular gas mass of 1.6×10^8 $M_\odot$ (Crocker et al. unpublished). No counterpart to this gas disc is detected in H I, implying that most of the cold ISM in the central regions of NGC 524 is in the form of molecular gas.

NGC 3032 - In this galaxy, a small regularly rotating H I disc is found, with a total H I mass of 9.7×10^7 $M_\odot$. The H I disc

co-rotates with the ionised gas observed (Sarzi et al. 2006), although the detail in the observed velocity field of the ionised gas is limited by binning effects. The molecular gas is found in a centrally concentrated rotating structure (Young, Bureau, & Cappellari 2008). The ionised, molecular and neutral gas are co-rotating. Interestingly, all these gaseous components are *counter-rotating* with respect to the bulk of the stars in this galaxy, strongly suggesting an external origin of the gas observed. Some stars have formed from this gas disc because McDermid et al. (2007) have found the presence of a small stellar core that is counter-rotating to the bulk of the stellar body (and hence co-rotating with the gas disc). The CO observations reveal a molecular gas reservoir of 2.5-$5.0 \times 10^8 M_\odot$(Combes et al. 2007; Young, Bureau, & Cappellari 2008). Thus, also in NGC 3032 most of the cold ISM is in the molecular phase.

NGC 3377/3379/3384–The Leo Group - The situation in NGC 3384 is very complex. This galaxy is member of the M96 group that is famous for its large H I ring encircling several galaxies of this group (the Leo Ring; Schneider et al. 1983). Subsequent to the observations reported here, we have imaged the H I over the entire region and a full study of the Leo Ring will be published elsewhere. One result of this work is that the Leo Ring appears to form a large spiral-like structure that appears to end very close, both in space and in velocity, to NGC 3384. At the endpoint of this spiral-like structure a fairly bright H I cloud is observed and this is the cloud we identify here with NGC 3384. However, it is conceivable that most of the H I of the Leo Ring originated from NGC 3384 (see Michel-Dansac et al. 2010). A complication is that the H I spiral appears to be interrupted by an interaction of the spiral galaxy NGC 3389 with the Leo Ring, modifying its structure. NGC 3389 has a long tail of H I observed at velocities about 600 km s^{-1} redshifted with respect to the H I shown in Fig. 1, but shows no optical signs of a tidal interaction.

NGC 3489 - In NGC 3489 we find an inner rotating H I structure aligned with the galaxy, as well as a low-column density tail. The total H I mass of this barred galaxy is $5.8 \times 10^6 M_\odot$. This galaxy might be in the process of accreting a small gas cloud or companion, and forming an inner disc from this material. The central H I structure shows regular rotation with the same sense of rotation as the ionised gas and the stellar component. Molecular gas with a mass of $1.2 \times 10^7 M_\odot$has been detected in this galaxy by Combes et al. (2007).

NGC 3608 - In the vicinity of NGC 3608 we detect a large H I structure, about 40 kpc in size and about 70 kpc from the galaxy. No H I was detected on NGC 3608 itself. A smaller H I cloud is also detected, closer to NGC 3608. Since the galaxy is a member of a loose group, the intergalactic H I clouds might reflect past interactions between the group members, but none of the nearby group galaxies hosts H I today. This field shows similarities with the elliptical galaxy NGC 1490 (Oosterloo et al. 2004) where a number of large H I clouds (with a total H I mass of almost $10^{10} M_\odot$) are observed that are lying along an arc 500 kpc in length and at a distance of 100 kpc from NGC 1490. The stars and the ionised gas in NGC 3608 are kinematically decoupled, at least in the centre, where the stars show a regular rotation pattern. No CO was found in this galaxy in the survey of Combes et al. (2007).

NGC 4262 - This strongly barred galaxy is the only object in a dense environment in which we detect in H I. The cold gas is distributed in a large ring. This ring shows regular rotation, albeit with signs of non-circular orbits. The observed structure is most likely a resonance ring due to the bar. The ionised gas rotates in the same sense as the H I whereas the stellar rotation is decoupled from that. No CO was detected by Combes et al. (2007).

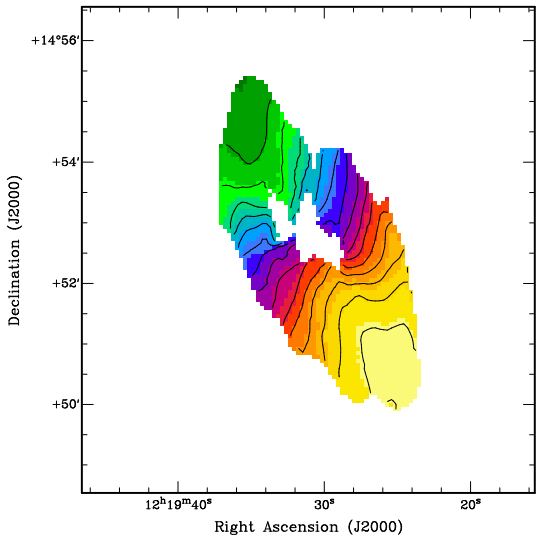

Figure 2. H I velocity field of NGC 4262. Iso-velocity contours run from 1160 km s^{-1} (top left) to 1510 km s^{-1} (bottom right) in steps of 25 km s^{-1}

4 DISCUSSION

Adding together the data from Morganti et al. (2006) and the present work, we have data cubes of 33 early-type galaxies from the representative *SAURON* sample of 48. Using this sample, we expand the analyses done in Morganti et al. (2006). In particular, we investigate here also the relation with the CO observations that have become recently available as well as the effect of environment on the presence of neutral hydrogen. We discuss the effect of the environment in Sec. 4.1 while in the rest of the discussion we focus on field galaxies, where the majority of the H I detections are found.

4.1 Environment

It is well established that the H I properties of spirals in clusters are strongly affected by the dense environment. Overall, spiral galaxies in clusters are deficient in H I compared to field spirals (e.g. Giovanardi, Krumm, & Salpeter 1983; Solanes et al. 2001, and refs therein), while imaging studies show that the H I discs in spirals in clusters are clearly affected by the dense environment (Cayatte et al. 1990; Oosterloo & van Gorkom 2005; Chung et al. 2009). The above studies have shown that dynamical interactions between galaxies, as well as stripping by the hot intracluster medium, are responsible for removing a large fraction of the neutral gas from cluster spirals. These mechanisms affect mainly the outer disc regions, because the inner gas discs in cluster galaxies have similar properties as those in field galaxies (Kenney & Young 1988; Young et al. 2010). Another important fact is that in the Virgo cluster the population of small, gas-rich galaxies that can be accreted by larger galaxies in smaller than in the field (Kent 2010). Therefore, galaxies entering a cluster not only lose gas, but they are also not able to replenish their gas supply by accreting companions. Therefore cluster galaxies become gas poor and remain so and will evolve into early-type galaxies.

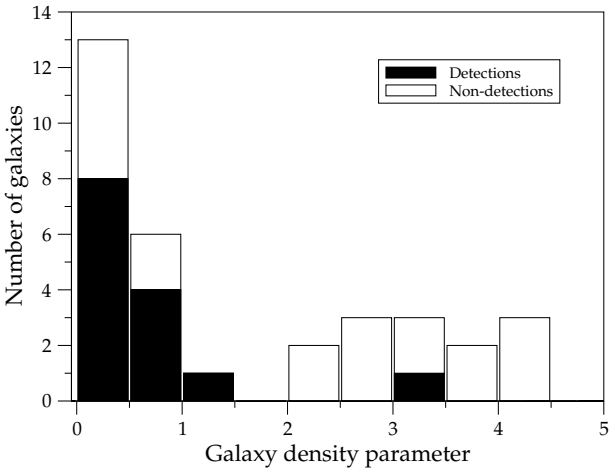

Figure 3. Distribution of the estimate of the local galaxy density as given in the NCG for galaxies detected and not detected in H I. Galaxies with galaxy density above 2 are member of the Virgo cluster

Given the above, one might expected that the H I properties of early-type galaxies strongly depend on the local galaxy density, even more so than for spirals. Observational evidence that this is indeed the case comes from studies based on the Arecibo Legacy Fast ALFA survey (ALFALFA Giovanelli et al. 2005). di Serego Alighieri et al. (2007) and Grossi et al. (2009) have used this survey to select early-type galaxies located in the Virgo cluster and in low density environments respectively. di Serego Alighieri et al. (2007) found a detection rate of only 2% for early-type galaxies that are member of the Virgo cluster. On the other hand, the detection rate for the early-type galaxies in low density environments (Grossi et al. 2009) is about ten times higher (25%). A similar contrast in H I properties has been observed by Serra et al. (2009). Although a simple division into cluster and field galaxies does not do justice to the wide range of H I properties observed in field galaxies (see below), our data, that moreover have a noise level about a factor 4 better than the ALFALFA data, strongly confirm the large difference in detection rates between galaxies in low and in high density environments. To illustrate this, we have divided our sample into cluster and field sub-samples and for the moment we ignore the wide range of the H I properties observed. To quantify the environment of our sample galaxies, we have used the estimates of their local galaxy densities given in the Nearby Galaxy Catalog (NGC, Tully 1988). This catalog gives, on a spatial grid of 0.5 Mpc, the density of galaxies brighter than –16 mag. Applying this information to our sample clearly separates it into low- and high-density sub-samples (see Fig. 3). The former sub-sample we will refer to as the field sample and the latter corresponds to galaxies in the Virgo cluster.

Figure 3 shows the distribution of the local galaxy density for galaxies not detected in H I and for galaxies where at least some H I was detected in or near the galaxy. This figure shows that only one object (NGC 4262) out of 13 cluster galaxies (8%) has been detected in H I, while in, or near, 14 of the 20 non-cluster galaxies (70%) at least some H I is detected, albeit with a large variety of H I properties ranging from small, off-centre clouds to large, regular H I discs. It is clear that, even with more sensitive observations, it is much more likely to detect H I in or near field galaxies than in or near Virgo early-type galaxies.

An important observation is that, as for Virgo spirals, the detection rate of *molecular gas* in early-type galaxies shows a much weaker environmental dependence (Combes et al. 2007; Young et al. 2010). Since these CO observations mostly refer to the central regions, this suggest that in early-type galaxies, gas removal, as in cluster spirals, occurs predominantly from their outer regions. The similarity of the effects of stripping suggest that gas removal is due to the same mechanism. The observation that the H I detection rate of early-type galaxies seems to be more affected than that of spirals is consistent with the fact that early-type galaxies form a more relaxed Virgo population than Virgo spirals (Binggeli, Tammann, & Sandage 1987). The different dynamical properties of the two populations suggest that early-type galaxies have been member of the Virgo cluster for a longer period and therefore may have suffered more from the environmental effects that remove gas from galaxies. Another effect can be that, compared to spirals, the H I in early-type galaxies is more often found in the outer regions of the galaxies so that it is more easily affected by interactions in the cluster.

Nevertheless, some of our detections in the field, e.g. NGC 3032 and NGC 3489, have their H I in an inner disc that could survive in the dense environment of Virgo. Still, such H I discs are not seen in our observations of Virgo galaxies. This could be explained if such inner discs in field galaxies are the remnants of relatively recent accretions (see also next section). The flat slope of the faint-end of the H I mass function observed for the Virgo cluster (Kent 2010) indicates that the population of small gas-rich objects, i.e. those objects that appear to supply field early-type galaxies with fresh gas, is smaller in the Virgo cluster than in the field. Therefore, once a Virgo early-type galaxy loses its gas through environmental effects, there is much less chance that a new supply of gas is accreted and once a Virgo early-type galaxy is H I poor, it will likely remain so, unlike galaxies in the field. Even if a gas-rich object accreted, interactions with the high density environment will more likely remove such gas during the accretion while it is still only loosely bound to the galaxy. That accretions in clusters are less gas rich is also observed for shell galaxies by Hibbard & Sansom (2003). The low gas accretion rate for cluster galaxies is also suggested by the observation that in several field galaxies we observe ongoing accretion, in stark contrast with the cluster galaxies, although the dense cluster environment implies a shorter time over which direct signs of interaction are visible. A lower detection rate of direct signs of ongoing interaction in clusters is also observed in other wave bands (e.g., Tal et al. 2009). Both gas removal and the lack of new gas supplies drive the morphological evolution of galaxies in the Virgo cluster from late type to early type.

4.2 Morphology of the H I in field early-type galaxies

The results of the previous section show that there is a large difference in overall H I properties between cluster and field early-type galaxies. However, as many earlier studies have shown, within the group of field early-type galaxies there is a very large range in H I properties and the situation with respect to H I in early-type galaxies is much more complex than just a simple division into cluster and field. Here we discuss this in some more detail.

Combining the results from Morganti et al. (2006) and the present work, we have deep H I images for 20 field early-type galaxies selected from the SAURON sample of 48. For 13 of these objects, we have detected H I in or near them. Figure 1, together with Fig. 1 from Morganti et al. (2006), shows that there is a very large range in properties of the H I structures in early-type galaxies, ranging from a single small cloud, to large, regular gas discs. Nevertheless, some overall trends can be seen and the morphology

and kinematics of the detected H I structures can be divided into 3 broad categories.

The first category (denoted C, for cloud) contains those objects where the H I is found in small clouds, where in some cases it is even not obvious whether the H I clouds are likely to be bound to the galaxy, or whether they are, e.g., "free-floating" remnants of a past interaction or even a low surface brightness companion. The galaxies that fall in this category are NGC 524, NGC 3384, NGC 3608, NGC 5982 and NGC 7332. The H I masses involved are small and are all less than a few times 10^7 $M_\odot$.

The second category (denoted A, for accretion) contains galaxies where the H I is found in unsettled structures that are clearly connected to a recent or an ongoing gas-rich accretion. The galaxies that fall in this category are NGC 1023, NGC 2768 and NGC 5198, while to some extent NGC 3489 could also fall in this category. The H I in NGC 1023 shows overall rotation, but the kinematics shows many irregularities and the H I is clearly not settled. The H I masses involved range from several times 10^6 $M_\odot$ to over 10^9 $M_\odot$.

The final category (denoted D, for disc/ring) refers to galaxies where most of the H I is found in a fairly regularly rotating disc or ring. This category contains the galaxies NGC 2685, NGC 3032, NGC 3414, NGC 3489, NGC 4150 and NGC 4278, while also the only cluster galaxy detected (NGC 4262) falls in this category. In NGC 2685 and in NGC 4278 the H I disc is large, i.e. extending beyond the bright optical body, while in NGC 3032, NGC 3489 and in NGC 4150 the H I forms a small, inner gas disc. In NGC 3414, the H I appears to form a polar ring or disc. For galaxies with discs, the H I masses involved range from several times 10^6 $M_\odot$ to over 10^9 $M_\odot$.

The first conclusion that can be drawn is that in about half the galaxies where H I is detected, it is found in a disc-like structure. Based on the first set of observations of the *SAURON* sample, Morganti et al. (2006) had found that gas discs appear to be common in early-type galaxies, while a similar result was found for early-type galaxies detected in the HIPASS survey (Oosterloo et al. 2007). The extended set of observations of the *SAURON* sample clearly confirms this.

The second conclusion is that accretion of gas is common in early-type field galaxies. For all galaxies detected the H I data reveal that accretion is on-going, or has occurred in the recent past. Galaxies with a gas disc also show clear signs of accretion: in NGC 3489, a faint, extended gas tail is detected which connects to the inner gas disc. Similarly, near NGC 4150 a small H I cloud is detected, while even the outer regions of the large, and presumably older, H I disc in NGC 4278 are connected to two large gas tails. The disc in NGC 2685 is heavily warped while the disc in NGC 3414 is polar, hence it is likely that also in these galaxies the gas has been accreted. The gas disc in NGC 3032 is counter-rotating to the stars. The conclusion is that gas discs in early-type galaxies form through accretion and that this is an ongoing process. Some of the variation we see in H I properties in our sample may be reflecting different stages of such accretion events. For example, NGC 2768 is accreting gas and a small inner polar disc is forming (Crocker et al. 2008). It is quite possible that this galaxy will evolve into a system similar to NGC 3414. The accretion and inner discs in NGC 3489 and NGC 4150 appear to have a similar history, where NGC 4150 is probably at a slightly more evolved stage. NGC 3032 may be at an even more evolved stage. Another example is NGC 1023 where a large and fairly massive H I structure is observed that shows an overall rotation pattern, but that clearly has not settled into a disc. This system may evolve into a galaxy with a large, regular gas disc, similar to the one seen in NGC 4278.

In a few galaxies, the amount of H I detected is above 10^9 $M_\odot$, i.e. similar to the amount of H I in the Milky Way. This suggests that in those cases the object accreted must have been fairly massive. Moreover, the large extent and regular disc kinematics indicate that some must have formed several Gyr ago. However, in most galaxies the H I masses involved are smaller and correspond to that of galaxies like the Magellanic Clouds or smaller. Assuming 10^9 yr for the timescale of a typical accretion (e.g. Sancisi et al. 2008; Tal et al. 2009), the detection rate and observed H I masses imply that the accretion rate for cold gas is smaller than 0.1 $M_\odot$ yr^{-1} for most field early-type galaxies. This suggests that, even allowing for the fact that the H I is only a fraction of the mass accreted, currently early-type galaxies grow only by a modest amount through accretion. This has to be the case because, although most galaxies are small in size, most of the mass in galaxies is already in large galaxies (Renzini 2006). Therefore there is no large enough reservoir of small galaxies available for large galaxies to grow substantially by accretion of companions. We note that only one galaxy (NGC 2685) shows clear optical peculiarities that can be associated with accretion (in this case polar dust lanes). This underlines that, although accretion often occurs, the mass of the accreted object is, in most cases, small compared to that of the host galaxy and the effects on the host galaxy usually are at most subtle. This is in line with optical imaging studies of other samples of early-type galaxies (e.g. Schweizer & Seitzer 1992; van Dokkum 2005; Tal et al. 2009) which have shown that most early-type galaxies in the field and in small groups show signs of small accretion events. The new aspect from our results is that small amounts of gas are involved in this continuing assembly of field early-type galaxies.

In a recent review, Sancisi et al. (2008) concluded that for at least 25% of field spiral galaxies there is direct evidence that a small gas-rich companion or gas cloud is accreting, or has been accreted in the recent past. Also for many of these objects the optical image does not show clear signs of interaction and the accretion is only visible in H I observations. It appears that, as far as the character of accretion is concerned, there is not much difference between field spiral galaxies and field early-type galaxies and to some extent, the H I properties of early-type galaxies bear a resemblance with those of the outer regions of spiral galaxies. Sancisi et al. (2008) estimate that, for field spiral galaxies, the accretion rate for cold gas is about 0.1 to 0.2 $M_\odot$ yr^{-1}, somewhat higher than we estimate for our early-type galaxies.

4.3 Dynamical structure of the host galaxies

Several theoretical studies have shown that the dynamical structure of a merger remnant critically depends on the amount of gas, and hence dissipation, present in (one of) the progenitors (e.g. Bender, Burstein, & Faber 1992; Jesseit, Naab, & Burkert 2005; Naab, Jesseit, & Burkert 2006; Hopkins et al. 2009; Jesseit et al. 2009). Moreover, a systematic change of the importance of dissipative effects as function of mass may explain the different dynamical properties of high-mass and low-mass early-type galaxies (Davies et al. 1983).

In Morganti et al. (2006) we had found that the H I detections are uniformly spread through the $(\epsilon, V/\sigma)$ diagram and we concluded, although the sample used was small, that if fast and slow rotators represent the relics of different formation paths, this did not appear to be reflected in the *current* characteristics of the H I. The discussion of the previous section showed that, except in a few

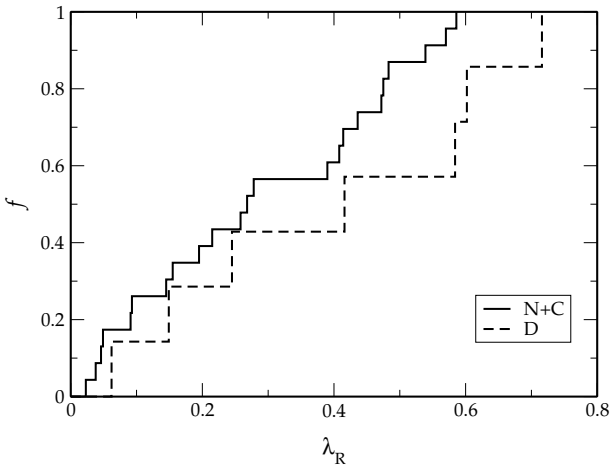

Figure 4. Cumulative distribution of $\lambda_{\rm R}$ for galaxies classified as having an H I disc (class D) compared with that for galaxies undetected in H I or where only a small H I cloud was detected (classes N and C).

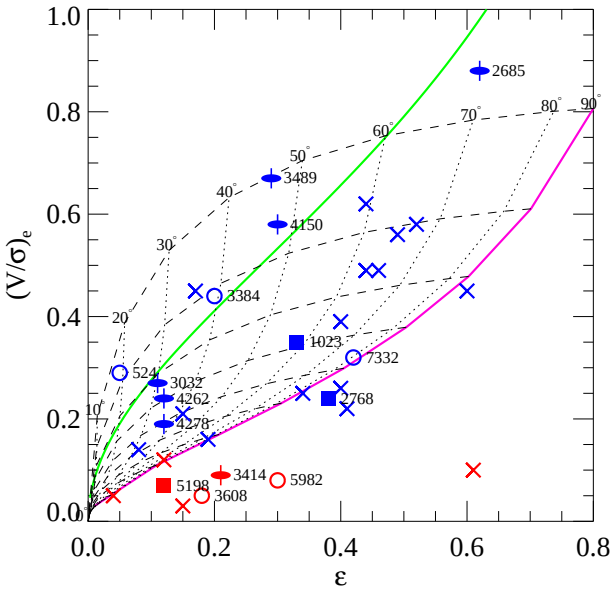

Figure 5. $(V/\sigma, \varepsilon)$ diagram for galaxies in our HI sample. Crosses are non detections, Ellipses with axis are are HI disks, Empty circles are isolated HI clouds and filled squares are HI accretion. Red/blue colours indicate slow/fast rotators. The NGC numbers of the HI detected galaxies are indicated. The magenta line corresponds to the relation $\delta = 0.7\varepsilon_{\rm intr}$ between anisotropy and intrinsic ellipticity. The dotted lines indicate how the relation is transformed when the inclination (indicated at the top) is decreased. The values are taken from (Cappellari et al. 2007), where a detailed explanation of the diagram is given.

cases, the H I currently detected is mainly due to recent small accretions. Because the dynamical structure of a galaxy is the result of the evolution over a Hubble time, a clear observable link with these recently accreted small amounts of gas may not be expected.

For our extended dataset there is, similar to the result of Morganti et al. (2006), not much evidence that, for most galaxies, the current H I content is connected to the dynamical characteristics of the galaxy. Different from Morganti et al. (2006), we use the parameter $\lambda_{\rm R}$, introduced by Emsellem et al. (2007) to describe the importance of rotation. This parameter involves luminosity weighted averages over the full two-dimensional stellar kinematic field as a proxy to quantify the observed projected stellar angular momentum per unit mass. It can have values between 0 and 1, and apart from projection effects, higher values of $\lambda_{\rm R}$ suggest that rotation is more important for the dynamics of the galaxy.

In Fig. 4 we show the cumulative distributions of $\lambda_{\rm R}$ for the group of galaxies that one could see as fast *gas* rotators (i.e. class D) and for the group of galaxies that are H I non- or slow gas rotators (classes N and C). No clear dichotomy emerges. For the discy H I detections, the distribution of $\lambda_{\rm R}$ appears to go to higher values, which would suggest that for some galaxies with an H I disc rotation is also important for the stellar component. On the other hand, there is good overlap for smaller values of $\lambda_{\rm R}$ suggesting that the presence of an H I disc is not a good discriminator. This is also suggested by, for example, the fact of the sixteen fast rotating field galaxies, only six have the H I distributed in a disk.

The *SAURON* galaxies were selected to sample uniformly the *projected* axial ratio and the E/S0 morphology. Both quantities are related to the galaxy inclination as is λ_R. For this reason the distribution of λ_R is related in a complex way to the selection criteria and it is difficult to interpret quantitatively. An alternative way to look at the relation between dynamics and H I morphology, while including possible inclination effects, is by using the $(V/\sigma, \varepsilon)$ diagram (Binney 2005). The study of the distribution of the *SAURON* galaxies on the diagram was discussed in Cappellari et al. (2007). It was shown that fast-rotators ETGs tend to lie in a restricted region of that diagram, defined at the lower boundary by a linear trend between intrinsic flattening and orbital anisotropy for edge-on systems (the magenta line in Fig. 5). Lowering the inclination moves galaxies to the left of that line on the $(V/\sigma, \varepsilon)$ diagram as illustrated in Fig. 5 (for a detailed explanation see Cappellari et al. (2007)). By plotting our different H I morphologies on the diagram we conclude that: (i) The galaxies with the fastest intrinsic (edge-on) V/σ in our sample all happen to posses H I disks. To these we should add NGC 2974, which has an intrinsic V/σ larger than NGC 3489 and also posses an H I disk (Weijmans et al. 2008). Within our limited number statistics this would suggests that an accretion/merger involving a large amount of gas is required to produce the galaxies most dominated by rotation; (ii) However the reverse is not true as H I disks can be present also at intermediate V/σ, which implies that H I disks do not necessarily produce a rotation-dominated object. A regular disk is seen in fact even in the slow rotators NGC 3414. Larger samples are needed to conclusively understand the link between H I and galaxy dynamics, but this work illustrates that there is not a simple connection.

4.4 H I and molecular gas

Atomic hydrogen is not the only tracer of the cold ISM in galaxies. A CO survey of the *SAURON* sample (Combes et al. 2007) has shown that a significant fraction of the *SAURON* galaxies contains molecular gas. It is therefore interesting to compare the H I properties of the *SAURON* galaxies with those of the CO. More recent observations (see Tab. 3) have somewhat modified the list of CO detections from Combes et al. (2007). The earlier CO detections in NGC 4278 and NGC 7457 have not been confirmed, while CO has now been detected in NGC 524. Of the sample we discuss in this paper, six galaxies are detected both in CO and in H I (NGC 524, NGC 2685, NGC 2768, NGC 3032, NGC 3489 and NGC 4150), out of a total of nine CO detections and fifteen H I detections. Interestingly, all these galaxies show small amounts of star formation (Shapiro et al. 2010, see also Sect. 4.6). In five of the CO detec-

NGC	H I type	$M_{\rm H_2}$ $M_\odot$	$M_{\rm H_2}/M_{\rm HI}$ central	CO references
(1)	(2)	(3)	(4)	(5)
524	none	1.6×10^8	>25.7	a
1023	dip	$<4.0 \times 10^6$	<0.6	b
2685	dip	2.1×10^7	12.2	c
2768	peak	6.8×10^7	8.5	d
3032	peak	5.0×10^8	11.1	e
3414	peak	$<9.0 \times 10^6$	<0.29	b
3489	peak	1.2×10^7	8.8	b
4150	peak	5.5×10^7	21.0	e
4262	dip	$<1.1 \times 10^7$	<2.32	b
4278	dip	$<6.4 \times 10^6$	<1.32	a
4459	none	1.6×10^8	>40.6	e
4477	none	2.4×10^7	>6.0	b
4550	none	7.2×10^6	>1.9	f

Table 3. Molecular mass to H I mass ratios for the galaxies with CO detections and/or central H I. (1) Galaxy identifier. (2) Classification of the central H I. (3) Total molecular gas mass. (4) Ratio of total molecular gas mass to the H I mass observed in the central interferometric beam. (5) References: (a) Crocker et al. unpublished; (b) Combes et al. (2007); (c) Schinnerer & Scoville (2002); (d) Crocker et al. (2008); (e) Young, Bureau, & Cappellari (2008) (f) Crocker et al. (in preparation).

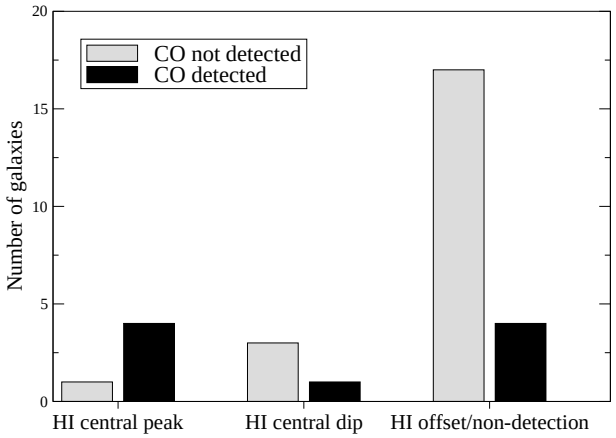

Figure 6. CO detection histogram as a function of central H I morphology.

tions H I is also seen in the central region of the galaxy (NGC 2685, NGC 2768, NGC 3032, NGC 3489, NGC 4150) and the CO and the H I show very similar kinematics, indicating that the same component is detected both in CO and H I. The exception is NGC 524 where no atomic counterpart is detected of the central molecular disc. Similarly, in the Virgo galaxies NGC 4459, NGC 4477 and NGC 4550 CO was found, but no H I.

For a proper comparison of the H I and the H_2 properties, it is important to keep in mind that the H I observations typically probe a region of several tens of kpc in size, i.e. an entire galaxy and its immediate environment, while the CO observations refer only to the central region of a galaxy on kpc scales. A comparison based on total H I content and a central CO measurement is not necessarily meaningful. The spatial resolution of our WSRT observations is well matched to the field-of-view of the IRAM 30-m dish used by Combes et al. (2007). We therefore compare the CO measurements with the H I detected in the single WSRT beam centred on the galaxy while taking into account the central morphology of the H I of our galaxies. We divided the central H I morphology in three categories: no central H I, central dip in the H I (within a large-scale H I structure), or central H I peak. The category for each galaxy is listed in Table 3 and the relation with the CO properties is given in Fig. 6. This figure clearly shows that a statistical relation exists between the presence of H I and CO in the central regions. Galaxies with centrally peaked H I are more likely to have CO than the other two types. Of the six galaxies with a centrally peaked H I distribution, five have a central CO component. For comparison, if one would use the total H I content, the statistics clearly gets diluted: of all fifteen H I detections, only six are detected in CO. We conclude that centrally peaked distributions of H I tend to harbour corresponding central molecular gas distributions. The only exception to this rule seems to be NGC 3414. However, the kinematics of the H I in this galaxy suggests that this H I likely forms an edge-on polar ring and that the observed central H I peak may be due to projection.

A few more things can be learned from this comparison. In the five galaxies where both H I and CO are detected in the central regions, interferometric CO observations (Crocker et al. 2008; Young et al. 2010; Crocker et al. 2010) show that the kinematics and the morphology of both components are clearly connected and the same physical structure is detected. A very nice example is the inner gas disc of NGC 3032 for which the extent and kinematics as seen in CO and in H I match exactly. A very interesting aspect is that the combination of the CO and H I observations of NGC 2768, NGC 3032, NGC 3489 and NGC 4150 gives clear evidence that these inner gas structures form by the accretion of small-gas-rich objects. The inner gas discs that are seen in NGC 2768, NGC 3489 and NGC 4150 connect to large, faint H I plumes that are seen at larger radii, clearly showing that these gas structures formed from accreted gas. The fact that the inner gas disc in NGC 3032 is counter-rotating to the stars also shows an external origin. Our results also show that the cold ISM of the inner gas discs detected both in H I and CO is mainly in the form of molecular gas, with the molecular gas mass being about 10 times higher than that of the atomic gas. Interestingly, this mass ratio is very similar to that seen in the centres of nearby spiral galaxies (e.g. Leroy et al. 2008), despite the very different state of the ISM in these two types of galaxies.

4.5 H I and ionised gas

With the new H I observations presented in this paper, we further confirm the result of Morganti et al. (2006) that galaxies with regular H I discs tend to have strong, extended emission from ionised gas that has the same kinematics as the H I while galaxies with unsettled H I structures have less ionised gas. For the galaxies for which we present data for the first time, regular discs of ionised gas are detected with *SAURON* in NGC 3032, NGC 3489 and NGC 4262 (Sarzi et al. 2006), exactly the three galaxies in the new observations in which regular H I discs are found. In the remaining H I detections, where the H I is found in small clouds offset from the centre (NGC 524, NGC 3384 and NGC 3608), only small amounts of ionised gas are detected. We therefore reiterate that, in early-type galaxies, a regular H I disc always has an ionised counterpart.

4.6 Neutral hydrogen and stellar population

Several earlier studies (e.g. Serra et al. 2006; Morganti et al. 2006) have concluded that the relation between H I content and stellar population for field early-type galaxies is complex. Our data show

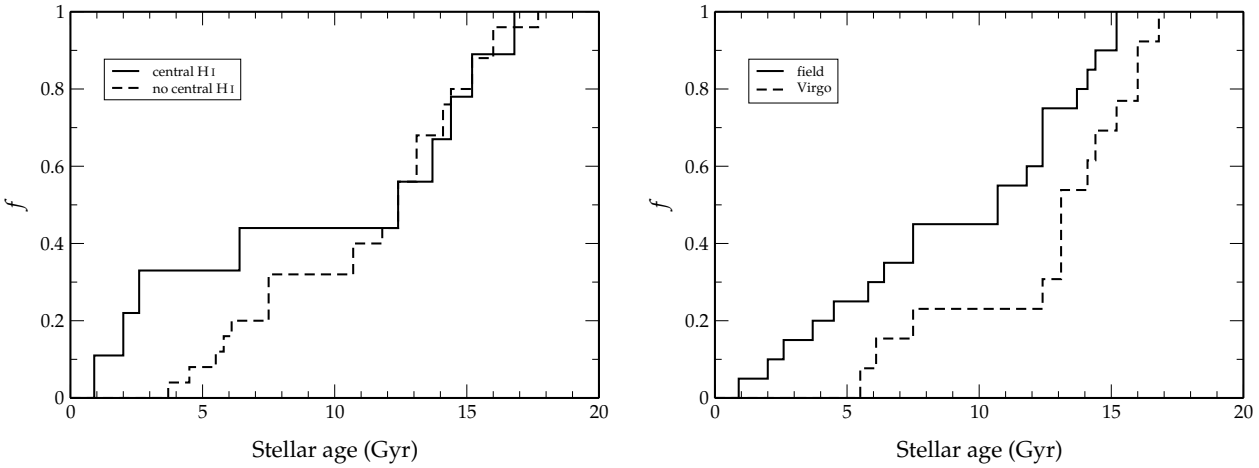

Figure 7. Left: cumulative distributions of stellar ages inside 1 R_e from single-population models from Kuntschner et al. (2010) where the sample is split in those galaxies with and those without H I detected in their central region. Right: Same distributions, but now the sample is split in field and Virgo galaxies

that, on the scale of the spatial resolution of our data, the column densities of the H I are below the threshold above which star formation is generally occurring. However, the highest column densities observed are not very much below this threshold, so given the low spatial resolution of our data, some star formation could occur in smaller regions. Low-level star formation (typically below levels of 0.1 $M_\odot$ yr^{-1}) is indeed observed in some of the gas-rich *SAURON* galaxies (Temi, Brighenti, & Mathews 2009; Jeong et al. 2009; Shapiro et al. 2010, see also below).

First we discuss to what extent the H I properties are connected to the ongoing star formation. As expected, some relation seems to hold. This is best illustrated by comparing our data with those from Shapiro et al. (2010). Based on *Spitzer* data, Shapiro et al. (2010), similarly to Temi, Brighenti, & Mathews (2009), observe small amounts of star formation in a subset of the *SAURON* galaxies. The star formation they observe only occurs in galaxies characterised by fast rotation. The morphology of the star forming regions is that of a thin disc or ring. Moreover, they were able to distinguish two modes of star formation. In one mode, star formation is a diffuse process and corresponds to widespread young stellar populations and high specific molecular gas content. Shapiro et al. (2010) associate this star formation with small accretion events. In the second mode, the star formation is occurring more centrally concentrated, while outside the region of star formation only old stellar populations are present. Smaller amounts of molecular gas are connected to these central star formation events. Shapiro et al. (2010) speculate that in at least some of these objects, the star are forming from gas resulting from internal mass loss.

It is interesting to see that in 4 of the 5 galaxies classified by Shapiro et al. (2010) to have widespread star formation and that are observed by us, both CO *and* H I is detected in the central regions (Table 3). In contrast, in none of the galaxies with centrally concentrated star formation H I is detected in the centre. This confirms the suggestion by Shapiro et al. (2010) that widespread star formation in early-type galaxies is connected with higher gas content. We do note that for some early-type galaxies *GALEX* data show that this relation between gas content and star formation also exists at *large* radius. Examples are NGC 404 (Thilker et al. 2010), NGC 2974 (Weijmans et al. 2008) and ESO 381–47 (Donovan et al. 2009). Almost all galaxies with widespread star formation and observed by us, have H I discs (NGC 2685, NGC 3032, NGC 3489, NGC 4150), quite distinct from galaxies with central star formation (no detection of NGC 4459 and NGC 4477, while only a small, offset H I cloud is detected in NGC 524). The only exception is NGC 4550, a galaxy in the Virgo cluster with widespread star formation and not detected in H I. This is a very unusual galaxy with two counter-rotating stellar discs. We also note that in all four galaxies with widespread star formation and detected by us, the H I is likely to have been accreted (see Sect. 4.2). This confirms the conclusion of Shapiro et al. (2010) that widespread star formation is associated with accretion.

The above results show that some star formation can occur in the gas reservoirs of early-type galaxies, although not all gas-rich galaxies show star formation. Overall, the connection with the properties of the stellar population is poor. Some galaxies indeed behave according to the expectation that the presence of a relatively large amount of H I indeed is connected to the properties of the stellar population, but the rule seems to be that for every rule there are exceptions. For example, NGC 1023, NGC 3414 and NGC 4278 have extensive reservoirs of neutral hydrogen, but do not show any evidence for the presence of a young stellar subpopulation. To characterise the overall stellar populations, we have used the single-population-equivalent stellar ages inside 1 $R_{\rm eff}$ as derived for the *SAURON* galaxies by Kuntschner et al. (2010). One way to investigate the connection between H I and stellar population is to compare these stellar ages of galaxies with H I to those of galaxies without central H I. In Fig. 7 we give the cumulative distributions of this stellar age for galaxies where H I is detected in the central regions and for those with no central H I. This figure suggests that some difference may exist between the two groups of galaxies, with some gas-rich galaxies having younger stellar ages. However, the difference between the distributions is mainly caused by only a few gas-rich galaxies that have quite young stellar ages (i.e. NGC 3032, NGC 3489 and NGC 4150 which are known to have ongoing star formation). Many galaxies with central H I have similar stellar populations as gas-free galaxies. Some galaxies with fairly young or intermediate ages are in fact gas free (e.g. NGC 3377 and NGC 7457) and some gas-rich galaxies have large stellar ages. A similar trend is seen when the total H I content is used instead of the central one. This is further illustrated in Fig. 8 where we plot the relative global gas content versus stellar age for the different H I morphologies. No clear overall trend is visible in this figure, except (again) that the three youngest galaxies all have a central H I disc that is also detected in CO. The at most weak connection be-

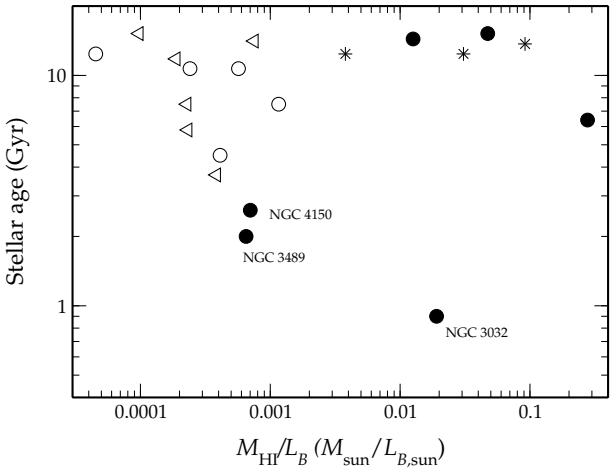

Figure 8. Stellar age inside 1 $R_{\rm eff}$ plotted as function of relative H I content. The different symbols refer to H I morphology: filled circles: regular disc/ring (class D); stars: unsettled H I structures (class A); open circles: small or offset H I clouds (class C); triangles: upper limits

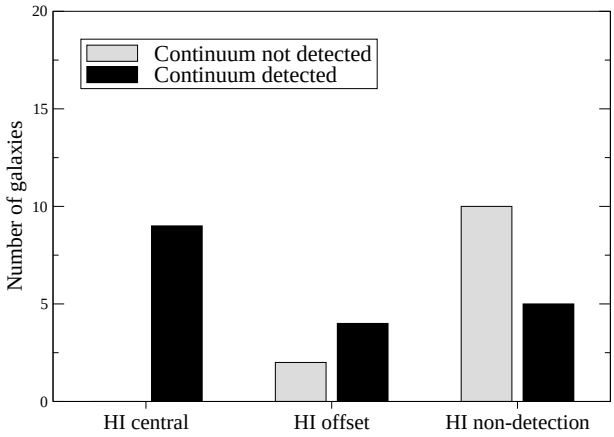

Figure 9. Histogram of the distribution of radio continuum detection as function of H I detection and morphology.

tween H I and stellar age is to a large extent similar to that seen for the ionised gas. Emsellem et al. (2007) show that those *SAURON* galaxies with relatively much ionised gas also have young stellar ages, but on the other hand several galaxies with young or intermediate age populations are free of ionised gas.

The results discussed above clearly show that the relation between H I and stellar populations is complex. This is not unexpected, since the stellar population is the result of the evolution of a galaxy over its entire life, while the current H I content only reflects the present state. In Sect. 4.2 we showed that some amounts of gas are accreted by field early-type galaxies at irregular intervals. Often the amounts of gas involved are small and, even if entirely converted into stars, will only leave subtle signatures in the stellar population that are not always easy to detect (see also e.g. Serra & Oosterloo 2010). Moreover, the efficiency with which accreted gas is turned into stars depends on many factors. For example, accretions characterised by loss of gas angular momentum (e.g., retrograde encounters) result in efficient gas infall that triggers central star formation. This may be observed as a young population in a relatively gas-rich galaxy, but after a while, the gas reservoir will be exhausted and the remnant is observed as H I-poor and centrally rejuvenated (Serra et al. 2006). On the other hand, interactions in which gas retains its angular momentum (e.g., prograde encounters) result in large H I tidal tails that can later be re-accreted to form large H I discs. Because of their large extent, the column densities in these discs is low and at most some star formation will occur in localised regions at large radius (see e.g. Oosterloo et al. 2007). Recent work also suggest that bulges can have a stabilising effect on discs, preventing star formation, even when significant amounts of gas is present (Martig et al. 2009).

It is instructive to consider the effect of the environment. The results discussed so far show that the relation between *current* gas content and stellar population is complex. However, by comparing the Virgo early-type galaxies with those in the field, one may get an idea of the effects of gas accretion over longer periods of time. Our data indicate that for field early-type galaxies, gas accretion does play a significant role in determining the stellar population. This can be seen by comparing the cumulative distributions of the stellar ages of Virgo and field galaxies (Fig. 7). These distributions show that there is a trend of field early-type galaxies, as a population, having younger stellar ages than Virgo early-type galaxies. This difference likely reflects the different long-term accretion history of the two groups of galaxies. Field early-type galaxies regularly accrete small amounts of gas from their environment and, over time, this leaves an observable signature in the stellar population. In contrast, galaxies in Virgo, being in a gas poor environment, grow much less by accretion of gas-rich companions and even if some gas is accreted, it is removed on a short timescale by the cluster environment. The stellar population of cluster early-type galaxies is much less rejuvenated during their evolution compared to field early-type galaxies.

4.7 H I and the radio continuum

As described in Sec. 2, our observations have also allowed to extract images of the radio continuum emission. As detailed below, these images are in many cases much deeper than those available so far. This resulted in a significant number of new detections of the radio continuum associated with our target galaxies. We detect radio continuum in 13 of the 20 field galaxies and in 5 of the 13 cluster galaxies. With the exception of a few well-known objects with strong radio continuum (e.g. NGC 4278, NGC 4374/M84), the majority of the detected sources have a radio flux of at most a few mJy. In all detected sources, the radio continuum comes from the central region of the galaxy.

The interesting result is that there appears to be a trend between detection of radio continuum and detection of H I in or around the galaxy. Figure 9 shows the distribution of radio continuum detections as function of H I presence and H I morphology. The histogram shows that the radio continuum detection rate is higher for objects where also H I is detected, with a suggestion of an additional trend that galaxies with H I but not in their central regions are less likely to be detected in radio continuum than galaxies with H I in the centre, but more likely than galaxies with no H I at all. This suggests that the cold gas somehow contributes in feeding the processes that produce the radio continuum emission in some galaxies. It is well known that both star formation and AGN activity can contribute to the radio continuum emission from early-type galaxies (Wrobel & Heeschen 1991). Here we address the question is to what extent the observed trend with HI properties is connected to radio emission from star formation or from radio-loud AGN.

To study this question, we estimated the radio continuum flux expected to be observed from the amounts of star formation seen by

Shapiro et al. (2010) and compared these with the observed fluxes. Of the 8 star forming galaxies overlapping between Shapiro et al. (2010) and us, 7 are detected in radio continuum. We used the relation given by Bell (2003) to convert star formation rates to radio luminosities. For NGC 2685, NGC 3032, NGC 3489, NGC 4150 and NGC 4459, the observed radio continuum flux matches, within the errors, what is expected from the observed star formation rates and we conclude that the observed radio continuum is associated with the star formation. NGC 524 is known to have a faint radio AGN (Nagar, Falcke, & Wilson 2005), and when correcting the observed radio flux for this AGN, also for this galaxy the observed radio continuum matches that what is expected based on the observed star formation rate. Our upper limit to the continuum flux of NGC 4550 is consistent with the observed star formation in this galaxy. Because Shapiro et al. (2010) derive the star formation rates from FIR data, the good match between predicted and observed radio continuum in these galaxies implies that they follow the well-known radio-FIR correlation. Only in one star forming galaxy (NGC 4477) is the observed radio flux much larger than expected (by about a factor 7), which most likely means that this galaxy harbours a radio loud AGN.

In the previous section, we showed that galaxies with H I in their central regions are more likely to have star formation, while here we find that in many of these star forming galaxies, the radio continuum detected is due to this star formation. For about half the galaxies represented in the first bin of Fig. 9 this is the case. On the other hand, for both other H I classes shown in this figure, only one of the objects is forming stars. These results show that the trend seen in Fig. 9 is at least partly due to enhanced star formation in galaxies with central H I.

The spatial resolution of our observations is relatively low (corresponding to a linear scale of the order of a kpc for the most distant galaxies). This makes it difficult to decide, based on the radio data alone, whether the observed radio continuum is due to a radio-loud AGN. We therefore have searched the literature for higher resolution radio continuum data.

One possibility is to look into the FIRST survey (Faint Images of the Radio Sky at Twenty-Centimeters Becker, White, & Helfand 1995). FIRST data have better spatial resolution ($\sim 5''$), but higher noise level (about 1 mJy beam^{-1}) compared to our WSRT observations. A search for detections in this survey has been also done by Sarzi et al. (2010). Of the 9 field galaxies detected by us at the level of a few mJy (i.e. such that the sensitivity of FIRST would allow to detect these sources) 7 are detected by FIRST. In only one of these detections - NGC 3032 - the radio emission is resolved by FIRST, suggesting the presence of star formation, consistent the results presented here on this galaxy.

More instructive is, however, to consider the work of Nagar, Falcke, & Wilson (2005, and references therein). Their work focuses on detecting radio nuclei with high brightness temperature ($> 10^7$ K) and/or jet-like structures as unambiguous indications for the presence of an AGN. They concentrated on low-luminosity active galactic nuclei (LLAGN) and AGN selected from the Palomar Spectroscopic sample of northern galaxies that they have studied at high frequency (15 G Hz) with the VLA ($0.15''$ resolution) and with VLBI at intermediate and high radio frequencies. At these high resolutions (corresponding to a linear size of a few tens of pc), they detect radio emission in almost 50 % of the sources, suggesting a high incidence of radio cores.

Interestingly, their sample includes a fair number of our objects, although, unfortunately, the sensitivity of their observations is not as good as of our WSRT observations (flux limit of 1-1.5 mJy for the VLA observations and 2.7 mJy for the VLBI observations). Of the galaxies that are in common, for 11 is our WSRT flux above their detection limit and *all* are detected in the high-resolution observations of Nagar et al., suggesting the presence of a compact (core?) structure in these galaxies. One further object (NGC 5198) is not included in the Nagar et al. list but is classified as AGN by Sarzi et al. (2010) and also this object is detected in radio (both by WSRT and by FIRST). Almost all these objects are observed not to have star formation (e.g. Shapiro et al. 2010). We conclude that many of our early-type galaxies harbour a radio-load AGN. Interestingly, these AGN are evenly distributed over the three H I classes used in Fig. 9 suggesting that AGN activity is not connected to whether there is cold gas in the central region of an early-type galaxy or not. The observed relation between central gas content and radio continuum seems therefore to be due to a higher probability for radio emission from star formation if a galaxy has a relatively large amount of gas in the central regions.

5 CONCLUSIONS

We have presented new, deep Westerbork Synthesis Radio Telescope observations of the neutral hydrogen in 22 nearby early-type galaxies selected from a representative sample of early-type galaxies studied earlier at optical wavelengths with the *SAURON* integral-field spectrograph. Combined with our earlier observations, this resulted in deep H I data on 33 nearby early-type galaxies. This is the largest homogeneous dataset of H I imaging data available for this class of objects.

In contrast to our earlier study (Morganti et al. 2006), this sample both covers field environments and the Virgo cluster. We find that the H I properties strongly depend on environment. For detection limits of a few times 10^6 $M_\odot$, we detect H I in about 2/3 of the field galaxies, while for Virgo galaxies the detection rate is $<$10%. This is consistent with earlier work (di Serego Alighieri et al. 2007; Grossi et al. 2009). We confirm earlier results (Morganti et al. 2006; Oosterloo et al. 2007) that in about half the early-type galaxies with H I, this atomic gas is in a regularly rotating H I disc or ring. In many objects, unsettled H I structures are detected, such as tails and clouds, sometimes connecting to a regular H I disc. This suggests that the gas discs form through accretion. We conclude that accretion of H I commonly occurs in field early-type galaxies, but typically with very modest accretion rates. In contrast, cluster galaxies do not accrete cold gas. All the H I discs that we observed have counterparts of ionised gas. Moreover, galaxies with an inner H I disc also have an inner molecular gas disc. The strikingly similar kinematics of these different tracers shows that they are all part of the same structure. The combination of H I and CO imaging clearly shows, through the detection of gas tails, that the inner discs are the result of accretion events. The cold ISM in the central regions is dominated by molecular gas ($M_{\rm H_2}/M_{\rm HI} \simeq 10$).

There is no obvious overall relation between current gas content and internal dynamics. This is not very surprising given that in most galaxies with H I it is due to the recent accretion of small amounts of gas while the dynamical characteristics are set over much longer timescales. Within our limited number statistics, the fastest rotating galaxies all posses H I disks. This would suggest that an accretion/merger involving a large amount of gas is required to produce the galaxies most dominated by rotation. However, the reverse is not true as H I disks can be present also at intermediate V/σ. The similarity between the kinematics of the H I and that of the stars seen in some of the galaxies with large, regular H I disks,

suggests that an accretion/merger involving a large amount of gas was part of the evolution of those systems.

We observe a close relationship between gas content and the small amounts of star formation which occurs in some of the *SAURON* galaxies. Galaxies with widespread star formation are gas rich and are galaxies that have experienced a recent accretion event. The radio continuum emission detected in these galaxies is consistent with the star formation observed. However, as already noticed by Morganti et al. (e.g. 2006) and Serra et al. (2006), the relation between H I and the overall properties of the stellar population is very complex. The few galaxies with a significant young sub-population and/or star formation, have inner gas discs. For the remaining galaxies there is no trend between stellar population and H I properties. Very interestingly, we find a number early-type galaxies that are very gas rich but are not forming stars and have not done so for a while as they only have an old stellar population. One example of such a galaxy is NGC 4278 where the fact that the large H I disc shows very regular kinematics implies that this galaxy has been gas rich for at least a few Gyr. Despite this, there is no evidence for a young stellar population in this galaxy. In addition, we find that the stellar populations of our field galaxies are typically younger than those in Virgo. This is expected because field galaxies are likely to have accreted some gas in the last few Gyr, while in the Virgo cluster this is not the case. The difference in stellar population is reflecting of the differences in accretion history of cold gas between the two groups of galaxies.

In about 50% of our sample, we detect a central radio continuum source. In many galaxies, the continuum emission is due to a radio-loud AGN, but continuum emission from star formation is also detected in some galaxies. Galaxies with star formation follow the radio-FIR correlation. The presence of radio continuum emission correlates with the H I properties, in the sense that galaxies with H I in the central region are more likely to be detected in continuum compared to galaxies without H I. Galaxies with H I but in off-centre structures behave in between. This trend is mainly due to the star formation observed in galaxies with central gas reservoirs, and is not related to AGN fuelling.

In this paper, we have presented a number of interesting trends that suggest that gas and gas accretion plays a role in the evolution of early-type galaxies, in particular those found in the field. Although our collection of H I images is the largest and deepest available for early-type galaxies, the number is still fairly small and the statistical basis for most of the trends we find is not strong. Similar data on larger samples will be needed to put the results presented here on a more solid basis. We are in the process of collecting deep H I imaging data for a much larger sample of early-type galaxies (the ATLAS^{3D} sample, see http://purl.org/atlas3d Cappellari et al. 2010; Serra et al. 2009) that will allow us to further investigate the trends described here.

ACKNOWLEDGMENTS

We thank the anonymous referee for helpful suggestions which improved the paper. The Westerbork Synthesis Radio Telescope is operated by the Netherlands Foundation for Research in Astronomy ASTRON, with support of NWO. This research has made use of the NASA/IPAC Extragalactic Database (NED) which is operated by the Jet Propulsion Laboratory, California Institute of Technology, under contract with the National Aeronautics and Space Administration. The Digitized Sky Survey was produced at the Space Telescope Science Institute under US Government grant NAG W-2166. MC acknowledge support from a STFC Advanced Fellowship (PP/D005574/1).

REFERENCES

Allen S. W., Dunn R. J. H., Fabian A. C., Taylor G. B., Reynolds C. S., 2006, MNRAS, 372, 21
Balmaverde B., Baldi R. D., Capetti A., 2008, A&A, 486, 119
Becker R. H., White R. L., Helfand D. J., 1995, ApJ, 450, 559
Bell E. F., 2003, ApJ, 586, 794
Bell E. F., et al., 2004, ApJ, 608, 752
Bender R., Burstein D., Faber S. M., 1992, ApJ, 399, 462
Bigiel F., Leroy A., Walter F., Brinks E., de Blok W. J. G., Madore B., Thornley M. D., 2008, AJ, 136, 2846
Binggeli B., Tammann G. A., Sandage A., 1987, AJ, 94, 251
Binney J., 2005, MNRAS, 363, 937
Briggs D. S., 1995, in Bulletin of the American Astronomical Society Vol. 27, High Fidelity Interferometric Imaging: Robust Weighting and NNLS Deconvolution. pp 1444
Cappellari M., et al., 2007, MNRAS, 379, 418
Cappellari M., et al., 2010, in prep
Cayatte V., van Gorkom J. H., Balkowski C., Kotanyi C., 1990, AJ, 100, 604
Chung A., van Gorkom J. H., Kenney J. D. P., Crowl H., Vollmer B., 2009, arXiv, arXiv:0909.0781
Combes F., Young L. M., Bureau M., 2007, MNRAS, 377, 1795
Crocker A. F., Bureau M., Young L. M., Combes F., 2008, MNRAS, 386, 1811
Crocker A. F. et al. in prep.
Davies R. L., Efstathiou G., Fall S. M., Illingworth G., Schechter P. L., 1983, ApJ, 266, 41
De Lucia G., Springel V., White S. D. M., Croton D., Kauffmann G., 2006, MNRAS, 366, 499
de Zeeuw P. T., Bureau M., Emsellem E., Bacon R., Carollo C. M., Copin Y., Davies R. L., Kuntschner H., Miller B. W., Monnet G., Peletier R. F., Verolme E. K., 2002, MNRAS, 329, 513
di Serego Alighieri S., et al., 2007, A&A, 474, 851
Donovan J. L., Hibbard J. E., van Gorkom J. H., 2007, AJ, 134, 1118
Donovan J. L., et al., 2009, AJ, 137, 5037
Emsellem E., Cappellari M., Peletier R. F., McDermid R. M., Bacon R., Bureau M., Copin Y., Davies R. L., Krajnović D., Kuntschner H., Miller B. W., de Zeeuw P. T., 2004, MNRAS, 352, 721
Emsellem E., et al., 2007, MNRAS, 379, 401
Giovanardi C., Krumm N., Salpeter E. E., 1983, AJ, 88, 1719
Giovanelli R., et al., 2005, AJ, 130, 2598
Grossi M., et al., 2009, A&A, 498, 407
Hibbard J. E., Sansom A. E., 2003, AJ, 125, 667
Hopkins P. F., Lauer T. R., Cox T. J., Hernquist L., Kormendy J., 2009, ApJS, 181, 486
Jeong H., et al., 2009, MNRAS, 398, 2028
Jesseit R., Naab T., Burkert A., 2005, MNRAS, 360, 1185
Jesseit R., Cappellari M., Naab T., Emsellem E., Burkert A., 2009, MNRAS, 397, 1202
Kaviraj S., Tan K.-M., Ellis R. S., Silk J., 2010, arXiv, arXiv:1001.2141
Kenney J. D., Young J. S., 1988, ApJS, 66, 261
Kennicutt Jr. R. C., 1989, ApJ, 344, 685
Kent B. R., 2010, AAS, 41, 386

Kereš D., Katz N., Weinberg D. H., Davé R., 2005, MNRAS, 363, 2
Kuntschner H., Emsellem E., Bacon R., Bureau M., Cappellari M., Davies R. L., de Zeeuw P. T., Falcón-Barroso J., Krajnović D., McDermid R. M., Peletier R. F., Sarzi M., 2006, MNRAS, 369, 497
Kuntschner H., 2010, MNRAS, submitted
Leroy A. K., Walter F., Brinks E., Bigiel F., de Blok W. J. G., Madore B., Thornley M. D., 2008, AJ, 136, 2782
Malin D. F., Carter D., 1983, ApJ, 274, 534
Martig M., Bournaud F., Teyssier R., Dekel A., 2009, arXiv, arXiv:0905.4669
McDermid R. M., et al., 2006, MNRAS, 373, 906
McDermid R. M., et al., 2007, NewAR, 51, 13
McNamara B. R., Sancisi R., Henning P. A., Junor W., 1994, AJ, 108, 844
Mei S., et al., 2005, ApJ, 625, 121
Michel-Dansac L., et al., 2010, ApJ, 717, L143
Morganti R., Sadler E. M., Oosterloo T., Pizzella A., Bertola F., 1997, AJ, 113, 937
Morganti R., de Zeeuw P. T., Oosterloo T. A., McDermid R. M., Krajnović D., Cappellari M., Kenn F., Weijmans A., Sarzi M., 2006, MNRAS, 371, 157
Naab T., Jesseit R., Burkert A., 2006, MNRAS, 372, 839
Nagar N. M., Falcke H., Wilson A. S., 2005, A&A, 435, 521
Nipoti C., Londrillo P., Ciotti L., 2003, MNRAS, 342, 501
Nipoti C., Treu T., Bolton A. S., 2009, ApJ, 703, 1531
Oosterloo T., Morganti R., Sadler E. M., Ferguson A., van der Hulst T., Jerjen H., 2004, IAUS, 217, 486
Oosterloo T., van Gorkom J., 2005, A&A, 437, L19
Oosterloo T. A., Morganti R., Sadler E. M., van der Hulst T., Serra P., 2007, A&A, 465, 787
Renzini A., 2006, ARA&A, 44, 141
Roberts M. S., Haynes M. P., 1994, ARA&A, 32, 115
Sage L. J., Welch G. A., 2006, ApJ, 644, 850
Sage L. J., Welch G. A., Young L. M., 2007, ApJ, 657, 232
Sánchez-Blázquez P., Gibson B. K., Kawata D., Cardiel N., Balcells M., 2009, MNRAS, 400, 1264
Sancisi R., Fraternali F., Oosterloo T., van der Hulst T., 2008, A&ARv, 15, 189
Sarzi M., Falcón-Barroso J., Davies R. L., Bacon R., Bureau M., Cappellari M., de Zeeuw P. T., Emsellem E., Fathi K., Krajnović D., Kuntschner H., McDermid R. M., Peletier R. F., 2006, MNRAS, 366, 1151
Sarzi M., et al., 2010, MNRAS, 402, 2187
Sault R. J., Teuben P. J., Wright M. C. H., 1995, ASPC, 77, 433
Schaye J., 2004, ApJ, 609, 667
Schinnerer E., Scoville N., 2002, ApJ, 577, L103
Schneider S. E., Helou G., Salpeter E. E., Terzian Y., 1983, ApJ, 273, L1
Schneider S. E., 1989, ApJ, 343, 94
Schweizer F., Seitzer P., 1992, AJ, 104, 1039
Serra P., Trager S. C., van der Hulst J. M., Oosterloo T. A., Morganti R., 2006, A&A, 453, 493
Serra P., Trager S. C., Oosterloo T. A., Morganti R., 2008, A&A, 483, 57
Serra P., et al., 2009, in: Panoramic Radio Astronomy: Wide-field 1-2 GHz research on galaxy evolution. Published online at http://pos.sissa.it/cgi-bin/reader/conf.cgi?confid=89, id.56
Serra P., Oosterloo T. A., 2010, MNRAS, 401, L29
Shapiro K. L., et al., 2010, MNRAS, 402, 2140
Solanes J. M., Manrique A., García-Gómez C., González-Casado G., Giovanelli R., Haynes M. P., 2001, ApJ, 548, 97
Tadhunter C., Robinson T. G., González Delgado R. M., Wills K., Morganti R., 2005, MNRAS, 356, 480
Tal T., van Dokkum P. G., Nelan J., Bezanson R., 2009, arXiv, arXiv:0908.1382
Temi P., Brighenti F., Mathews W. G., 2009, ApJ, 707, 890
Thilker D. A., et al., 2010, ApJ, 714, L171
Trager S. C., Faber S. M., Worthey G., González J. J., 2000, AJ, 119, 1645
Tonry J. L., Dressler A., Blakeslee J. P., Ajhar E. A., Fletcher A. B., Luppino G. A., Metzger M. R., Moore C. B., 2001, ApJ, 546, 681
Tully R. B, 1988, *Nearby Galaxy Catalog* (NGC), Cambridge University Press, Cambridge
van Dokkum P. G., 2005, AJ, 130, 2647
van Driel W., van Woerden H., 1991, A&A, 243, 71
Weijmans A.-M., Krajnović D., van de Ven G., Oosterloo T. A., Morganti R., de Zeeuw P. T., 2008, MNRAS, 383, 1343
Welch G. A., Sage L. J., 2003, ApJ, 584, 260
Wrobel J. M., Heeschen D. S., 1991, AJ, 101, 148
Yi S. K., et al., 2005, ApJ, 619, L111
Young L. M., Bureau M., Cappellari M., 2008, ApJ, 676, 317
Young L. M. et al. in prep.